

# Study on the Effect of Torrefaction on Pyrolysis Kinetics and Thermal Behavior of Cornstalk Based On a Combined Approach of Chemical and Structural Analyses

Xincheng Lu, Ruting Xu, Kang Sun, Jianchun Jiang,\* Yunjuan Sun, and Yanping Zhang



Cite This: *ACS Omega* 2022, 7, 13789–13800

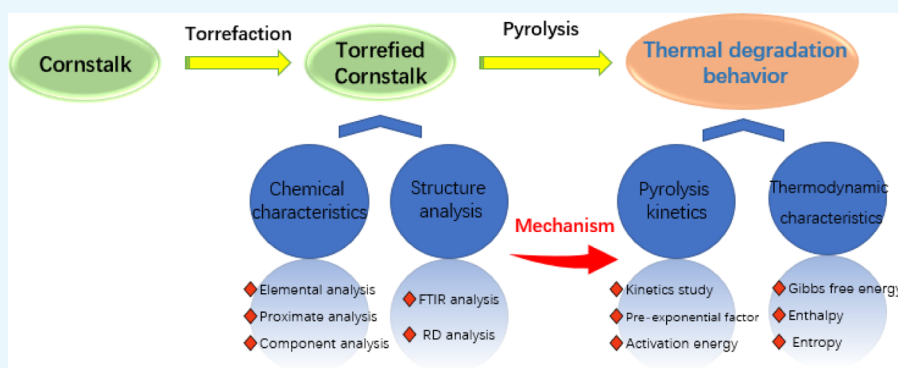


Read Online

ACCESS |

Metrics & More

Article Recommendations



**ABSTRACT:** In this study, the effects of torrefaction pretreatment on physicochemical characteristics and pyrolysis behavior of cornstalk were investigated based on the changes in its chemical and structural characteristics. The results indicated that torrefaction treatment improved the fuel properties with elevated torrefaction temperature, including the lower volatile content, higher carbon content, and higher heating value. In addition, serious torrefaction promoted complete degradation of hemicellulose, while the lignin was increased obviously. The crystallinity degree of cornstalk increased first and then reduced with the torrefaction temperature. Slight torrefaction enhanced the devolatilization and thermochemical reactivity of cornstalk, but serious torrefaction discouraged the volatile release. Kinetic parameter analysis indicated that the Ozawa–Flynn–Wall model was more accurate in calculating the activation energy, and the average activation energy gradually increased from 196.06 to 199.21, 203.17, and 217.58 kJ/mol. Furthermore, the thermodynamic parameters also showed an increasing trend with elevated torrefaction temperature. These results provide important basic data support for the thermochemical conversion of cornstalk to energy and chemicals.

## 1. INTRODUCTION

Powered by population growth and economic development, the demand for energy is continuously increasing every year. At present, the energy sources are mainly fossil fuel-based and non-renewable, which cause resource depletion and serious environmental problems.<sup>1</sup> Therefore, the application of renewable and clean energy sources has attracted more attention and is regarded as an effective way to solve the energy problem. Among all the renewable energy sources, lignocellulosic biomass is considered as the most viable substitution to fossil energy due to its renewability and abundant reserves.<sup>2,3</sup> Agricultural residues are the main sources of lignocellulosic biomass. As one of the most abundant agricultural residues in China, nearly 330 million tons of cornstalk is produced in a year. Utilization of cornstalk for power and fuel production could reduce the pollution emission and provide more job opportunities as well.

Pyrolysis, as one kind of thermochemical conversion technologies, is widely used in converting biomass into fuels or chemicals, which involves the thermal decomposition of biomass to produce gas, solid, and liquid products.<sup>4</sup> However, there are some disadvantages of raw biomass limiting its utilization, such as the low energy density, high water content, and difficulty in grinding. Therefore, the pretreatment of biomass before pyrolysis has attracted extensive attention. Torrefaction refers to heat treatment at lower temperatures of 200–300 °C in an inert atmosphere, which has been recognized as a promising way to improve the physicochemical

**Received:** January 4, 2022

**Accepted:** March 16, 2022

**Published:** April 18, 2022



properties and pyrolysis behavior of biomass.<sup>5</sup> Chen et al. revealed the torrefaction mechanism of biomass components, which provided an essential theoretical support in this field.<sup>6</sup> Tapasvi et al. found that torrefaction reduced the contents of water and oxygen in the biomass and improved the grindability and energy density.<sup>7</sup> Chen et al. indicated that torrefaction enhanced the cellulose content in biomass and decreased the oxygen content in the bio-oil obtained from biomass pyrolysis with the increase of torrefaction temperature.<sup>8</sup> Furthermore, torrefaction changes the composition and structure of biomass, which affects the pyrolysis characteristics and kinetics. Ru et al. investigated the effects of torrefaction on pyrolysis behavior of polar wood and found that torrefaction showed significant influence on its physicochemical characteristics and pyrolysis behavior.<sup>9</sup>

For utilization of cornstalk by pyrolysis on a substantial scale, kinetic analysis using thermograms is essential, which are conducive to determining the kinetic parameters and investigating the reaction mechanism. In addition, kinetic analysis provides the information needed for optimizing the process parameters and designing a pyrolysis reactor, and it also provides information on mathematical modeling simplification.<sup>10</sup> Thermogravimetry analysis (TGA) is the most common method used for pyrolysis kinetic analysis.<sup>11</sup> During TGA, the slow heating rate leads to a certain weight loss for the isothermal method before reaching the presupposed pyrolysis temperature, which causes the deviation on the kinetic parameters estimation. Therefore, a non-isothermal method is more time-saving and reliable, which includes a model-free (isoconversion) method and model-fitting method. The iso-conversion method, such as Kissinger–Akahira–Sunose (KAS) and Ozawa–Flynn–Wall (OFW), can calculate the activation energy without understanding the mechanism.<sup>12</sup>

Despite various remarkable research studies having been carried out to study the biomass pyrolysis kinetics, there are no data available to investigate the reaction kinetics and pyrolysis mechanism of cornstalk. In addition, there is also a lack of studies on the effect of torrefaction on the pyrolysis kinetics and thermal behavior of cornstalk. Therefore, this study was performed to study the effects of torrefaction pretreatment on the cornstalk pyrolysis kinetics and thermodynamics and to investigate the influence of the mechanism, which could provide a good reference for the thermal application of cornstalk. In this study, three different temperatures (210, 240, and 270 °C) were used to torrefy the cornstalk, and four different heating rates (5, 10, 20, and 30 °C/min) were selected to discuss the pyrolysis kinetic performance. The basic characteristics were analyzed and the changes in the chemical structures of cornstalk were characterized by Fourier transform infrared (FTIR) spectroscopy and X-ray diffraction (XRD). In addition, the iso-conversion methods, the KAS method and the OFW method, were used to study the pyrolysis kinetics and thermodynamic properties. The variation of pyrolysis behavior was explained based on the changes in chemical and structural characteristics, which help to reveal the influence of torrefaction on cornstalk pyrolysis.

## 2. MATERIALS AND METHODS

**2.1. Materials.** Cornstalk (CS) was used as the raw material in this study and collected from the surrounding countryside of Zhengzhou, China. Before the experiment, the cornstalk was cut into 1–2 cm size and then dried at 105 °C for 24 h.

**2.2. Torrefaction Pretreatment.** The torrefaction pretreatment was carried out in a fixed-bed reactor. 20 g of dried cornstalk was added into a quartz tube and then placed in the center of the fixed-bed reactor. N<sub>2</sub> was fed into it with a flow rate of 300 mL/min to provide an inert environment. The sample was heated to the desired temperature (210, 240, and 270 °C) with a heating rate of 10 °C/min and maintained for 60 min, which are then marked as CS-210, CS-240, and CS-270. Each torrefaction pretreatment was repeated three times to ensure the experimental repeatability.

**2.3. Sample Characterization.** **2.3.1. Biomass Characterization.** The proximate analysis (ash content, volatile content, and fixed carbon content) was carried out according to the National Standard of China GB/T 28731-2012. The elemental analysis was performed using a PerkinElmer elemental analyzer (PerkinElmer 2400, Germany). The obtained results were presented as percentages of C, H, N, and S, and the O content was determined by the difference. The wet chemistry method of Van Soest was used to determine the chemical composition of the sample (hemicellulose, cellulose, and lignin).<sup>12,13</sup> HHV was calculated according to the Dulong formula.<sup>14</sup>

$$\text{Heating value (MJ/kg)} \\ = 0.338C + 1.428(H - O/8) + 0.095S \quad (1)$$

The mass yield, energy yield, and energy density were calculated using the following equations

$$\text{mass yield (\%)} = \frac{M_T}{M_R} \times 100\% \quad (2)$$

$$\text{energy density} = \frac{HHV_T}{HHV_R} \quad (3)$$

$$\text{energy yield} = \frac{M_T \times HHV_T}{M_R \times HHV_R} \times 100\% \quad (4)$$

where  $M_R$  and  $M_T$  represent the mass of raw and torrefied samples, respectively, and  $HHV_R$  and  $HHV_T$  represent the higher heating values of raw and torrefied samples, respectively.

**2.3.2. FTIR Analysis.** An FTIR spectrometer (IS10, Niko, USA) was used to investigate the chemical structure of the sample. 1 mg of sample and 300 mg of dry KBr were mixed uniformly and then pressed into a tablet. The IR spectra were acquired between 4000 and 500 cm<sup>-1</sup>. The height values and peak areas of bands were used to represent the relative changes in the chemical structure of the sample.

**2.3.3. XRD Analysis.** An X-ray diffractometer (D8 FOCUS, Bruker, Germany) was used to analyze the cellulose crystallinity of the sample. Analysis was conducted using Cu K $\alpha$  radiation ( $\lambda = 0.154$  nm) and scanning was done from 10 to 40° at 40 kV/40 mA with a step of 0.02°/s. The crystallinity index (CrI), representing the percentage of crystalline cellulose, was calculated by Segal's method (eq 5) to investigate the effect of torrefaction pretreatment on the crystallinity of sample.<sup>15</sup>

$$\text{CrI(\%)} = \frac{I_{200} - I_{am}}{I_{200}} \times 100\% \quad (5)$$

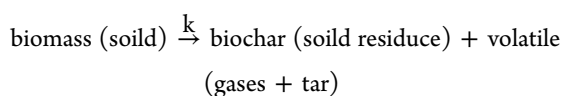
where  $I_{200}$  is the intensity of the (200) peak at  $2\theta = 22.5^\circ$  representing both amorphous and crystalline intensities and  $I_{am}$  is the intensity of the amorphous peak at  $2\theta = 18^\circ$ .

**2.3.4. TG Analysis.** The pyrolysis behavior of the sample was tested by a TG analyzer (TG–differential TG (DTG), 409PC, Netzsch, Germany). In the experiment, N<sub>2</sub> (99.999%) with a flow rate of 40 mL/min was used to provide an atmosphere. 10 mg samples were used in each experiment, and the experiment temperature was from 40 to 800 °C with the heating rates of 5, 10, 20, and 30 °C/min. The devolatilization index was defined and used to reveal the release performance of volatile components in the sample during the pyrolysis process.<sup>16</sup>

$$D_1 = \frac{R_{\max}}{T_i \times T_{\max} \times \Delta T_{1/2}} \quad (6)$$

where  $R_{\max}$  is the maximum decomposition rate,  $T_i$  is the initial devolatilization temperature,  $T_{\max}$  is the maximum mass loss temperature,  $\Delta T_{1/2}$  is the temperature interval when the value of  $R/R_{\max}$  is 1/2, and  $R$  is the decomposition rate.

**2.4. Kinetic Methods.** The pyrolysis of biomass is a complicated process. Considering its complicity, the total pyrolysis reaction mechanism of biomass can be expressed as the following overall mechanism<sup>17</sup>



Assuming the conversion of raw materials into the product is a one-step process, the reaction rate constant ( $k$ ) according to the Arrhenius equation can be represented by the following equation

$$k = Ae^{-\frac{E}{RT}} \quad (7)$$

where  $k$ ,  $A$ ,  $E$ ,  $R$ , and  $T$  refer to the reaction rate constant, pre-exponential factor ( $\text{min}^{-1}$ ), activation energy ( $\text{kJ mol}^{-1}$ ), gas constant ( $8.314 \text{ J mol}^{-1}$ ), and absolute temperature (K), respectively. For the process of converting biomass from the solid state to the volatile state, the rate equation can be expressed as

$$\frac{dx}{dt} = kf(x) \quad (8)$$

where  $x$  is the conversion rate within the sample and can be defined as

$$x = \frac{\alpha_0 - \alpha_t}{\alpha_0 - \alpha_f} \quad (9)$$

where  $\alpha_0$  is the initial weight of biomass,  $\alpha_t$  is the mass of biomass at a particular time, and  $\alpha_f$  is the mass of biomass at the end of pyrolysis process. According to eqs 7 and 8, we get

$$\frac{dx}{dt} = Ae^{-\frac{E}{RT}}f(x) \quad (10)$$

According to the  $n$ -level uniform kinetic reaction,  $f(x)$  can be represented as

$$f(x) = (1 - x)^n \quad (11)$$

According to eqs 10 and 11, we get

$$\frac{dx}{dt} = Ae^{-\frac{E}{RT}}(1 - x)^n \quad (12)$$

$\delta$  is the heating rate (K/min) and can be defined as

$$\delta = \frac{dT}{dt} = \frac{dT}{dx} \times \frac{dx}{dt} \quad (13)$$

Combining eqs 12 and 13, we get

$$\frac{dx}{dT} = \frac{A}{\delta} e^{-\frac{E}{RT}}(1 - x)^n \quad (14)$$

Then, eq 14 can be converted into

$$\frac{dx}{(1 - x)^n} = \frac{A}{\delta} e^{-\frac{E}{RT}} dT \quad (15)$$

Integrating both sides of eq 15 simultaneously and let the left side as  $g(x)$ , we get

$$g(x) = \int_0^x \frac{dx}{f(x)} = \int_0^T \frac{A}{\delta} e^{-\frac{E}{RT}} dT \quad (16)$$

$$g(x) = \frac{AE}{\delta R} \int_{u_0}^u u^{-2} e^{-u} du = \frac{AE}{\delta R} p(u) \quad (17)$$

where  $u = E/RT$ . Because  $p(u)$  has no exact solution, it needs to be solved by a numerical approximation.<sup>18</sup>

**2.4.1. KAS Model.** As a model-free method, KAS can be used to calculate the kinetic energy of the material. By applying the approximation of  $p(u) = u^{-2}e^{-u}$  in eq 11, we get

$$\ln\left(\frac{\delta}{T^2}\right) = \ln\left[\frac{AR}{Eg(x)}\right] - \frac{E}{RT} \quad (18)$$

In this eq,  $x$  can be specified as a value, and temperature  $T$  can be obtained from the TGA curve with different heating rates. The apparent activation energy ( $E$ ) can be calculated from a plot of  $\ln(\delta/T^2)$  versus  $1/T$  for the given slope.

**2.4.2. OFW Model.** The OFW model is one of the most widely used methods to calculate pyrolysis kinetics, which used a correlation of heating rate, inverse temperature, and activation energy. The model proposes an empirical equation for  $p(u)$

$$\log(e^{-u}u^{-2}) = -2.315 - 0.4567u \quad (u > 20) \quad (19)$$

Substituting eq 16 and  $u = E/RT$ , we get

$$\log(\delta) = \log\left[\frac{AE}{Rg(x)}\right] - 2.315 - 0.4567\frac{E}{RT} \quad (20)$$

The activation energy can be obtained from the slope of the straight line of  $\log(\delta)$  versus the inverse temperature  $1/T$ .

**2.5. Pre-exponential Factor and Thermodynamic Parameters.** A model-free non-isothermal method was developed by Kissinger to calculate the pre-exponential factor, and the final equation is represented as

$$A = \frac{\delta E e^{\frac{E}{RT_{\max}}}}{RT_{\max}^2} \quad (21)$$

The thermodynamic parameters, such as the enthalpy change  $\Delta H$ , Gibbs free energy  $\Delta G$ , and entropy change  $\Delta S$ , can be calculated using the activated complex theory of Eyring.

$$\Delta H = E - RT_{\max} \quad (22)$$

$$\Delta G = E + RT_{\max} \ln\left(\frac{K_B T_{\max}}{Ah}\right) \quad (23)$$

$$\Delta S = \frac{\Delta H - \Delta G}{T_{\max}} \quad (24)$$

where  $K_B$  is the Boltzmann constant ( $1.381 \times 10^{-23} \text{ m}^2 \cdot \text{kg} / \text{s}^2 \cdot \text{K}$ ), and  $h$  is the Planck constant ( $6.626 \times 10^{-34} \text{ m}^2 \cdot \text{kg} / \text{s}$ ).

### 3. RESULTS AND DISCUSSION

#### 3.1. Characterization of Raw and Torrefied Cornstalk.

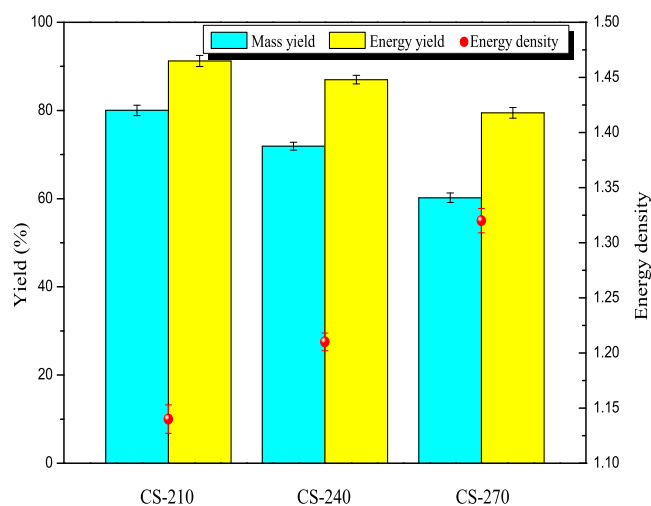
**3.1.1. Basic Characteristic Analysis.** The elemental analysis, proximate analysis, and component analysis of raw and torrefied cornstalk are presented in Table 1. It can be seen that the volatile content (V) decreased obviously from 78.48 to 59.58% with the increase of torrefaction temperature. On the contrary, the fixed carbon content (FC) increased from 18.21 to 35.59%. As shown in elemental analysis, with the increase of temperature, the C content increased from 43.15 to 55.22%, while the O content reduced from 47.00 to 34.00%. The removal of oxygen indicated that deoxygenation was the main reaction during the torrefaction process. The effect of torrefaction on the H and N contents was not obvious. According to component analysis, torrefaction pretreatment showed remarkable influence on the chemical composition of cornstalk. For raw cornstalk, the contents of hemicellulose, cellulose, and lignin were 15.48, 36.41, and 10.55%, respectively. After torrefaction, the hemicellulose content reduced, while cellulose and lignin contents increased. Due to poor thermal stability, the hemicellulose almost completely decomposed by torrefaction at 270 °C. Lignin is the most thermally stable component and its content increased obviously after torrefaction. For CS-270, the contents of hemicellulose, cellulose, and lignin were 0.26, 47.68, and 44.61%, respectively. In addition, the HHV also increased, due to the changing chemical composition and increasing energy density.

Figure 1 shows the effect of torrefaction pretreatment on the mass yield, energy yield, and energy density of cornstalk. As is shown, the mass yield and energy yield of torrefied cornstalk decreased with the increase of torrefaction temperature. The mass yield and energy yield decreased from 80.03 to 60.21% and 91.23 to 79.48% with the torrefaction temperature increasing from 210 to 270 °C, respectively. On the contrary, the energy density increased from 1.14 to 1.32 with the temperature increasing from 210 to 270 °C. Hence, torrefaction treatment could obviously improve the fuel properties of cornstalk, including a lower volatile content, higher carbon content, HHV value, and energy density.

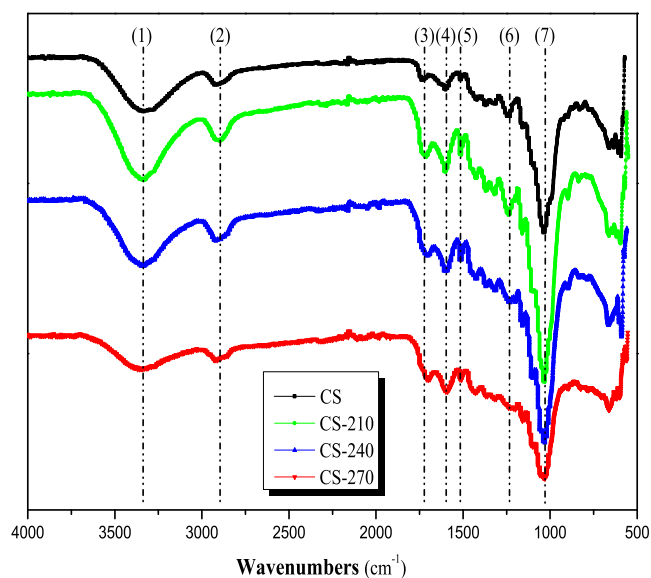
**3.1.2. Structure Analysis.** FTIR analysis of samples is shown in Figure 2. On the basis of literature, the significant characteristic absorption bands in the FTIR spectra can be divided into several regions:<sup>19,20</sup> (1) 3200–3500  $\text{cm}^{-1}$  is the stretching vibration peak of the O–H bond; (2) 2850–2970  $\text{cm}^{-1}$  is the stretching vibration peak of the C–H bond; (3) 1720–1738  $\text{cm}^{-1}$  is mainly attributed to the C=O bond in hemicellulose; (4) 1640–1655  $\text{cm}^{-1}$  and (5) 1507–1514  $\text{cm}^{-1}$  are the C=C vibration peaks of benzene ring in lignin; (6) 1263–1269  $\text{cm}^{-1}$  is assigned to C–O stretching in lignin; and (7) 1060–1039  $\text{cm}^{-1}$  is the stretching vibration peak of the C–O bond in cellulose and hemicellulose. It can be seen that torrefaction showed a significant influence on the chemical structure of cornstalk. Compared with the raw cornstalk, the adsorption peak of the O–H bond enhanced slightly after torrefied at 210 °C. With the increase of torrefaction temperature, the adsorption peak of the O–H bond gradually weakened, which may be due to the dehydration reaction that occurred during the torrefaction process, and promoted the removal of aliphatic hydroxyl groups in hemicellulose and

Table 1. Basic Characteristic Analysis of Samples

sample	elemental analysis (%)			proximate analysis (%)			component analysis (%)			HHV (MJ/kg)	
	C	O	H	N	V	FC	A	hemicellulose	cellulose		lignin
CS	43.15 ± 0.38	47.00 ± 0.51	5.90 ± 0.03	0.64 ± 0.01	78.48 ± 0.96	18.21 ± 0.38	3.31 ± 0.08	15.48 ± 0.57	36.41 ± 0.62	10.55 ± 0.18	14.04 ± 0.11
CS-210	48.55 ± 0.62	41.07 ± 0.39	5.38 ± 0.10	0.77 ± 0.03	72.12 ± 0.53	23.65 ± 0.64	4.23 ± 0.04	5.34 ± 0.31	41.39 ± 0.84	27.91 ± 0.41	16.00 ± 0.18
CS-240	51.32 ± 0.28	37.87 ± 0.23	5.04 ± 0.04	1.05 ± 0.05	67.64 ± 1.09	27.64 ± 0.86	4.72 ± 0.11	0.52 ± 0.09	45.74 ± 1.08	42.05 ± 0.92	16.94 ± 0.33
CS-270	55.22 ± 0.81	34.00 ± 0.46	4.76 ± 0.17	1.19 ± 0.03	59.58 ± 0.92	35.59 ± 1.05	4.83 ± 0.51	0.26 ± 0.08	47.68 ± 0.95	44.61 ± 0.78	18.53 ± 0.36



**Figure 1.** Mass yield, energy yield, and energy density of torrefied cornstalk.



**Figure 2.** FTIR spectra of raw and torrefied cornstalk.

cellulose. In addition, the adsorption of C–H bond also weakened with the elevated torrefaction temperature. During the torrefaction process, the demethylation and demethylene reactions occurred to the xylan unit in hemicellulose and the glucose unit in cellulose, resulting in the decrease of C–H.<sup>2</sup> A similar variation trend was observed in the C–O bond in cellulose and hemicellulose. Compared with raw cornstalk, the C=C vibration peak representing the benzene ring of lignin in torrefied cornstalks was enhanced significantly, indicating that the content of lignin could be increased by torrefaction. These changes in the structure suggested that torrefaction reduced the hemicellulose content but increased the cellulose and lignin contents, which are consistent with the component analysis details presented in Table 1.

Figure 3 shows the XRD patterns of samples with different torrefaction treatments. According to the literature, the diffraction angles ( $2\theta$ ) at  $14.80$ – $15.30^\circ$ ,  $16.20$ – $16.30^\circ$ ,  $18.30$ – $18.40^\circ$ , and  $21.90$ – $22.70^\circ$  were assigned as (110) crystallographic plane, (110) crystallographic plane, amorphous phase, and (200) crystallographic plane, respectively.<sup>21</sup>

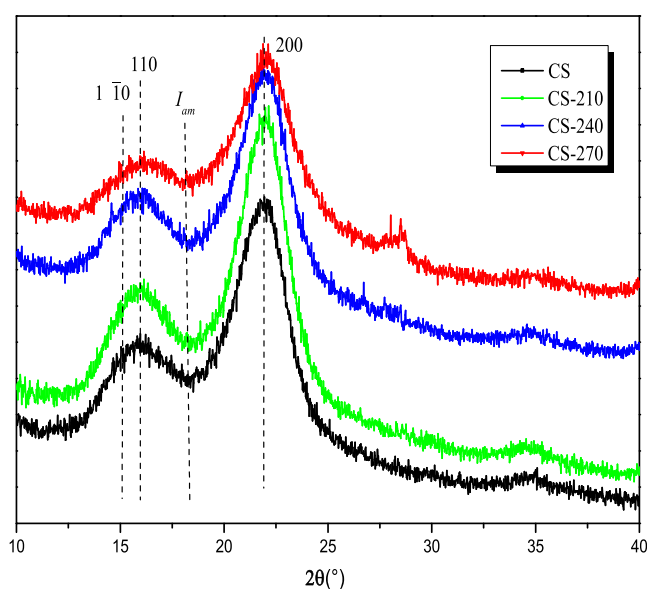


**Figure 3.** XRD patterns of raw and torrefied cornstalk.

It can be seen that torrefaction exhibited obvious effects on the (110) crystallographic plane, amorphous phase, and (200) crystallographic plane. Compared with the raw material, the absorption intensity of (110) and (200) crystallographic planes increased while the amorphous phase decreased. This indicated that torrefaction pretreatment destroyed the amorphous phase of cellulose and increased the crystallinity. With the increase of torrefaction temperature, the absorption intensity of (110) and (200) crystallographic planes reduced, indicating the decrease of crystallinity. The CrI calculated from eq 2 is as follows: 38.56% for CS, 45.51% for CS-210, 42.72% for CS-240, and 35.86% for CS-270. During the torrefaction pretreatment, at lower torrefaction temperatures, the amorphous components of cornstalk (such as hemicellulose and the amorphous phase of cellulose) decomposed, while most of the crystalline components of cellulose remained, thus increasing the crystallinity; moreover, the amorphous cellulose recrystallized, which was more likely to thermally decompose compared to crystalline cellulose, causing the increase of crystallinity.<sup>22</sup> However, when the torrefaction temperature was increased further, it changed the hydrogen bonds between the cellulose molecules and caused the crystalline cellulose to gradually degrade into amorphous cellulose, resulting in the decrease of crystallinity.<sup>4</sup>

**3.2. Pyrolysis Behavior.** **3.2.1. TG/DTG Analysis.** The TG and DTG curves of raw and torrefied samples are presented in Figure 4. The TG curves revealed that the pyrolysis of samples involved three main stages: desiccation stage ( $<180^\circ\text{C}$ ), devolatilization stage ( $180$ – $450^\circ\text{C}$ ), and char formation stage ( $>450^\circ\text{C}$ ). For raw cornstalk, the desiccation stage resulted in the removal of residual water and lower-molecular-weight compounds. The devolatilization stage is the main process in pyrolysis, and the mass loss was nearly 65%, which was due to the decomposition of hemicellulose and cellulose. The char formation stage was assigned to the pyrolysis temperature higher than  $450^\circ\text{C}$ , and the mass loss decreased which was associated with the decomposition of lignin. For the torrefied cornstalk, pyrolysis behavior was similar to that of raw cornstalk, but the temperature range has a significant change. Comparing the TG and DTG curves, it can be seen that

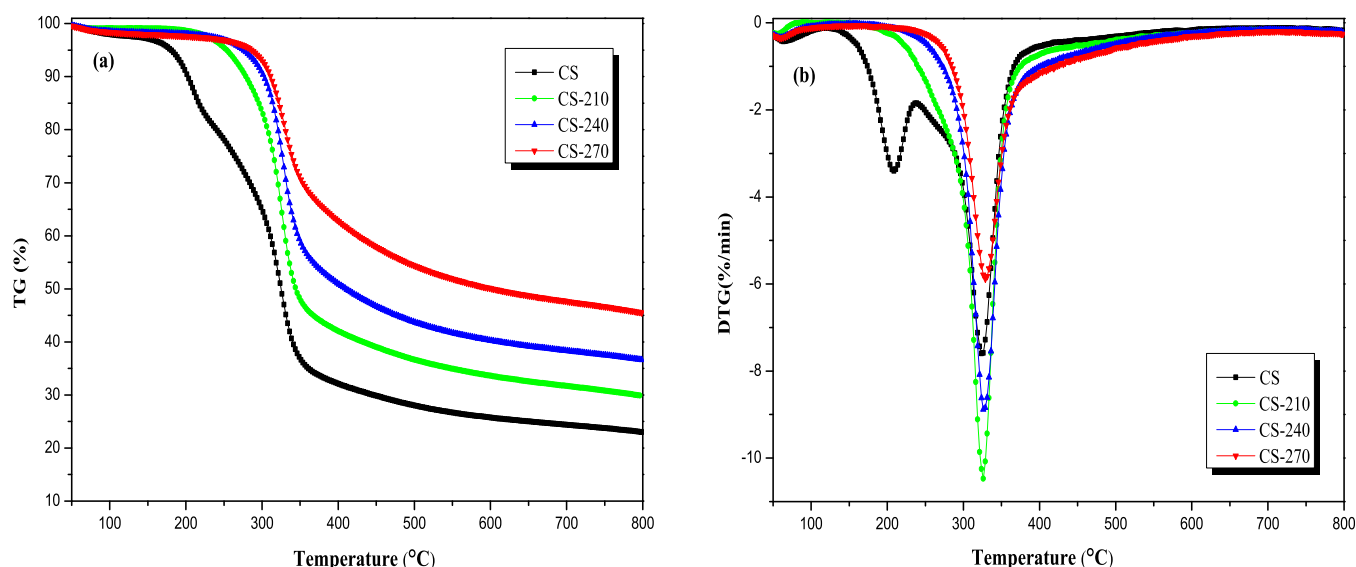


**Figure 4.** TG and DTG curves of raw and torrefied cornstalk. (a) TG curve and (b) DTG curve.

torrefaction increased the initial pyrolysis temperature and reduced the mass loss. In addition, the shoulder peak (around 200 °C) in DTG curves almost disappeared after torrefaction, which confirmed the decrease of the hemicellulose content by torrefaction. It can be seen from Table 2 that the initial

**Table 2. Pyrolysis Characteristic Parameters of Raw and Torrefied Cornstalk**

samples	$T_i$ (°C)	$T_{max}$ (°C)	$DTG_{max}$ (%/min)	residue (wt %)	mass loss (wt %)
CS	182.4	322.5	-7.73	24.04	75.96
CS-210	295.4	326.4	-9.76	31.70	68.30
CS-240	302.2	326.5	-9.68	36.61	63.39
CS-270	303.4	328.9	-6.51	44.15	55.85

pyrolysis temperature ( $T_i$ ) and the maximum weight loss rate temperature ( $T_{max}$ ) increased with the increase of torrefaction temperature. Moreover, the mass loss of pyrolysis decreased, while the residual mass increased. Torrefaction pretreatment decreased the content of hemicellulose and increased the contents of cellulose and lignin, thus improving the thermal stability of biomass and causing the increase of  $T_i$  and  $T_{max}$ . In addition, the polycondensation of lignin enhanced the thermal stability of lignin and led to the increase of  $T_f$ . The maximum weight loss rate ( $DTG_{max}$ ) increased first after torrefaction and reached the highest value of 9.76%/min at a torrefaction temperature of 210 °C. As the temperature was increased further, the structure of cellulose changed and the crystallinity reduced, resulting in the obvious decrease of  $DTG_{max}$ .<sup>4</sup> The residue increased after torrefaction, which was mainly due to torrefaction that caused an increase in the lignin content, promoted the polymerization of lignin's benzene ring unit, and enhanced the aromaticity of cornstalk.<sup>23</sup>

**3.2.2. Effect of Heating Rate on Biomass Decomposition.** The pyrolysis curves of samples at different heating rates are shown in Figure 5. As can be seen, the TG and DTG curves shifted to a higher temperature with the increase of the heating rate. In general, biomass has poor thermal conductivity and result in a thermal hysteresis (temperature gradient) in the whole cross section during the pyrolysis process.<sup>24</sup> At a lower heating rate, it is assumed that the temperature curve along the

biomass cross section has a linear relationship with the outer surface, and the inner core of the biomass reaches the same temperature at a specific time if the heating time is sufficient. However, at a higher heating rate, the temperature distribution of the inner core and the surface along the biomass section is significantly different and therefore forms a thermal hysteresis.<sup>25</sup> As can be seen from Table 3, the  $T_i$  and  $T_{max}$  increased gradually with the increase of heating rate. For raw cornstalk, when the heating rate increased from 5 to 30 °C/min, the  $T_i$  increased from 173.8 to 223.2 °C, and the  $T_{max}$  increased from 313.0 to 342.9 °C. Moreover, the conversion rate ( $x$ ) increased from 0.64 to 0.68. This increasing trend also can be found in the torrefied cornstalk. Those results confirmed that the total volatile products increased with the increase of the heating rate. The biomass pyrolysis process and degradation reaction kinetics are complex, and it may generate a resistance at a low heating rate; while at a high heating rate, the resistance could be overcome due to the high mass and heat transfer, resulting in a higher conversion.<sup>24</sup> Besides, Table 3 indicates that the residual mass increased with the increase of the heating rate. Chutia et al. reported that the lower heating rate provided higher heat transfer, which promoted the decomposition of biomass and resulted in less residual mass. While at the higher heating rate, a thermal hysteresis was formed between the biomass, which promoted the formation of coke and caused the increase of residual mass.<sup>26</sup>

The devolatilization index ( $D_i$ ) includes the effect of  $T_i$ ,  $T_{max}$ , and  $R_{max}$ , which can be used to describe the volatile property of biomass during the pyrolysis process.<sup>27,28</sup> The larger  $D_i$  value means the higher release of volatile matter and the better pyrolysis performance. The effect of heating rate on the  $D_i$  value is shown in Figure 6. It can be seen that the  $D_i$  value increased gradually with the increase of heating rate. In addition, the  $D_i$  value increased first with the elevated torrefaction temperature and reached the highest value at 210 °C and then decreased as the torrefaction temperature was increased further. This indicated that slight torrefaction promoted the volatile release of biomass and enhanced the thermochemical reactivity and devolatilization performance, while serious torrefaction discouraged the volatile release and biomass pyrolysis.

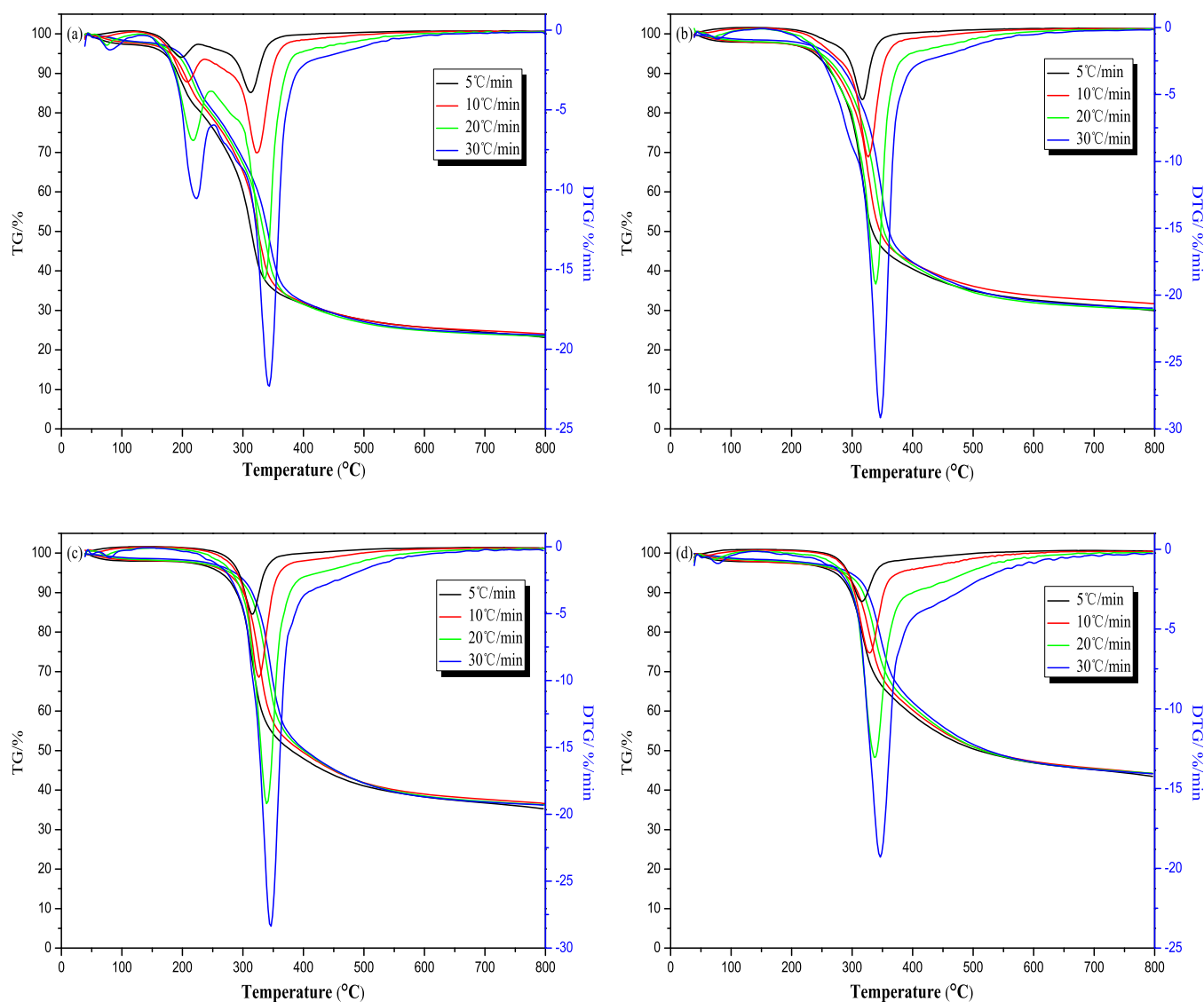


Figure 5. TG/DTG curves of samples at different heating rates: (a) CS, (b) CS-210, (c) CS-240, and (d) CS-270.

Table 3. Pyrolysis Characteristic Parameters of Samples at Different Heating Rates

samples	heating rate (°C/min)	$T_i$ (°C)	$T_{max}$ (°C)	DTG <sub>max</sub> (%/min)	$\alpha$	residue (wt %)
CS	5	173.8	313.0	-3.92	0.64	23.15
	10	182.4	322.5	-7.73	0.65	24.04
	20	218.1	335.9	-15.63	0.67	24.42
	30	223.2	342.9	-22.37	0.68	25.75
CS-210	5	285.2	317.1	-5.40	0.52	29.91
	10	254.4	326.4	-9.76	0.54	31.70
	20	300.7	338.9	-19.18	0.56	32.15
CS-240	5	290.6	315.4	-5.05	0.42	35.22
	10	302.2	326.5	-9.68	0.42	36.61
	20	313.0	339.6	-19.22	0.45	37.26
CS-270	5	289.9	316.1	-3.27	0.36	43.36
	10	303.4	328.9	-6.51	0.37	44.15
	20	311.6	337.7	-13.08	0.37	44.20
	30	318.3	346.5	-19.30	0.38	45.12

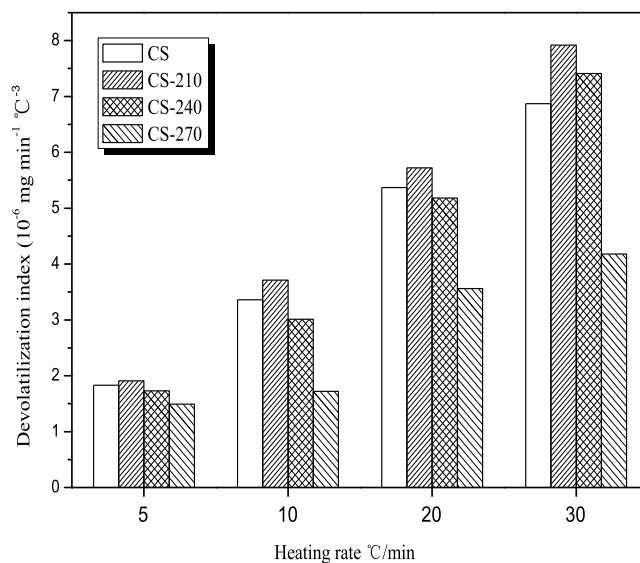
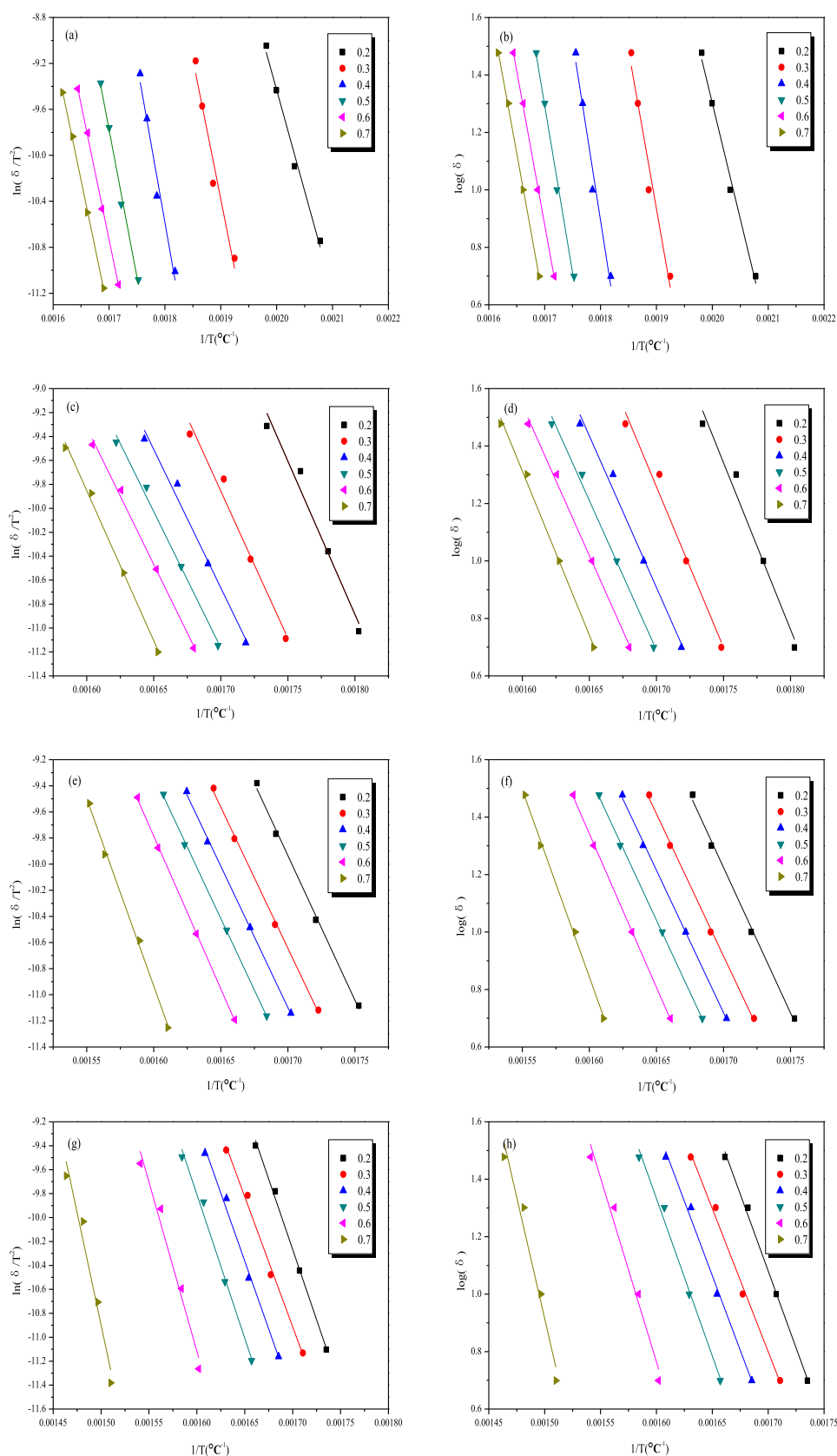


Figure 6. Effect of heating rate on  $D_i$ .



**Figure 7.** Kinetic plot for raw and torrefied cornstalk. (a) CS using the KAS method, (b) CS using the OFW method, (c) CS-210 using the KAS method, (d) CS-210 using the OFW method, (e) CS-240 using the KAS method, (f) CS-240 using the OFW method, (g) CS-270 using the KAS method, and (h) CS-270 using the OFW method.

**3.3. Pyrolysis Kinetics Analysis.** The KAS method and OFW method are widely used to determine the kinetic

parameters and investigate the pyrolysis behavior. The TG data were analyzed by the KAS method and OFW method, and the

Table 4. Kinetic Parameters of Thermal Degradation of Raw and Torrefied Cornstalk

samples	$x$	KAS model		OFW model	
		$R^2$	$E$ (kJ/mol)	$R^2$	$E$ (kJ/mol)
CS	0.20	0.9849	145.91 ± 2.31	0.9864	146.54 ± 1.54
	0.30	0.9489	202.82 ± 2.21	0.9529	201.23 ± 1.44
	0.40	0.9647	229.05 ± 2.67	0.9673	226.66 ± 1.32
	0.50	0.9906	213.17 ± 2.15	0.9913	211.91 ± 1.09
	0.60	0.9981	195.52 ± 2.31	0.9982	195.34 ± 1.75
	0.70	0.9988	194.62 ± 1.54	0.9990	194.63 ± 1.99
	average		196.85 ± 0.92		196.06 ± 1.21
CS-210	0.20	0.9644	212.91 ± 1.81	0.9674	211.41 ± 3.28
	0.30	0.9688	204.51 ± 1.92	0.9716	203.71 ± 1.22
	0.40	0.9814	192.06 ± 3.98	0.9832	192.05 ± 1.55
	0.50	0.9905	189.32 ± 0.91	0.9915	189.56 ± 0.72
	0.60	0.9941	190.21 ± 2.63	0.9945	190.50 ± 1.87
	0.70	0.9942	213.72 ± 2.17	0.9948	208.02 ± 2.16
	average		200.46 ± 1.78		199.21 ± 1.32
CS-240	0.20	0.9959	204.25 ± 2.21	0.9963	204.44 ± 1.94
	0.30	0.9980	199.64 ± 1.19	0.9982	200.22 ± 1.45
	0.40	0.9987	189.71 ± 2.09	0.9988	190.40 ± 4.04
	0.50	0.9991	191.84 ± 1.66	0.9992	192.53 ± 1.72
	0.60	0.9995	194.36 ± 1.72	0.9996	194.56 ± 0.78
	0.70	0.9959	238.58 ± 1.93	0.9962	236.88 ± 1.13
	average		203.07 ± 1.47		203.17 ± 1.24
CS-270	0.20	0.9859	199.78 ± 2.50	0.9873	199.74 ± 2.59
	0.30	0.9947	195.38 ± 1.50	0.9953	195.11 ± 3.43
	0.40	0.9889	188.43 ± 2.87	0.9900	188.79 ± 1.54
	0.50	0.9901	180.72 ± 3.32	0.9911	181.31 ± 1.56
	0.60	0.9654	235.01 ± 1.38	0.9683	233.55 ± 2.50
	0.70	0.9500	311.69 ± 1.95	0.9534	307.03 ± 2.51
	average		218.50 ± 1.15		217.58 ± 1.79

kinetic plot fitting curves are shown in Figure 7. Because the KAS and OFW methods do not involve the reaction order in calculating activation energy and do not affect the analysis results, the reaction order  $n = 1$  was selected for this study to calculate the kinetic parameters following many research studies.<sup>29,30</sup> As can be seen from Figure 6, the fitting curves of TG data showed good linearity, indicating that the KAS and OFW models had good fitting performance on pyrolysis behavior and were suitable to calculate the activation energy between the conversion rate of 0.2–0.7. The calculated activation energy ( $E$ ) and the respective correlation factor ( $R$ ) using KAS and OFW methods resulted in the conversion rate of 0.2–0.7, which are listed in Table 4. The correlation coefficients ( $R^2$ ) were higher than 0.95 for two models, and the  $R^2$  of the OFW model was higher than that of the KAS model, indicating that the OFW model was more accurate in calculating the activation energy. Activation energy is considered as the minimum energy required to cause the reaction, and a higher activation energy indicates a slower reaction.<sup>12</sup> As can be seen from Table 4, the conversion rate exhibited a significant effect on activation energy. For raw cornstalk, the activation energy increased gradually when the conversion rate increased from 0.20 to 0.40 and then decreased for a conversion rate higher than 0.50. After torrefaction, the change in the activation energy showed an opposite trend to that of raw cornstalk. In addition, the average activation energy calculated by the KAS method was slightly higher than that of the OFW method. The average activation energy of raw cornstalk was 196.06 kJ/mol, while that of torrefied samples were 199.21, 203.17, and 217.58 kJ/mol. This indicated that

torrefaction promoted the increase of activation energy, which positively correlated with the torrefaction temperature. Pyrolysis is a complex process involving multiple reactions and relates to the biomass composition, such as hemicellulose, cellulose, and lignin. In general, the activation energy of three components in the descending order is lignin, cellulose, and hemicellulose.<sup>31,32</sup> After torrefaction, the decomposition of hemicellulose and the partial decomposition of cellulose led to lignin becoming the main component and increased the activation energy. In addition, the increase in activation energy indicated the increase of the thermal stability of the sample, which was consistent with the increase of  $T_i$  with elevated torrefaction temperature. During the torrefaction process, the decomposition of cellulose became more concentrated and increased the driving force of mass transfer of volatiles, thus increasing the activation energy.<sup>22</sup> Therefore, torrefaction pretreatment altered the composition and chemical structure of the biomass, affected the dispersion of volatilization, diffusion, and heat transfer mechanism, and then changed the pyrolysis behavior.

**3.4. Thermodynamic Parameters.** In general, enthalpy ( $\Delta H$ ), Gibbs free energy ( $\Delta G$ ), and entropy ( $\Delta S$ ) represent the total heat capacity of a system. Previous studies indicated that the thermodynamic parameters, such as  $\Delta H$ ,  $\Delta G$ , and  $\Delta S$ , showed no significant change at different heating rates during pyrolysis.<sup>10</sup> Table 5 presents the thermodynamic parameters of raw and torrefied cornstalk at a heating rate of 10 °C/min. It can be seen that the thermodynamic parameters calculated by KAS and OFW methods exhibited the same variation trend, but the values were different. As revealed by kinetic analysis,

Table 5. Thermodynamic Parameters of Raw and Torrefied Cornstalk at 10 °C/min

X	KAS model				OFW model			
	A (min <sup>-1</sup> )	$\Delta H$ (kJ·mol <sup>-1</sup> )	$\Delta G$ (kJ·mol <sup>-1</sup> )	$\Delta S$ (J·mol <sup>-1</sup> ·K <sup>-1</sup> )	A (min <sup>-1</sup> )	$\Delta H$ (kJ·mol <sup>-1</sup> )	$\Delta G$ (kJ·mol <sup>-1</sup> )	$\Delta S$ (J·mol <sup>-1</sup> ·K <sup>-1</sup> )
CS								
0.20	3.09 × 10 <sup>12</sup>	140.96 ± 2.36	152.80 ± 3.41	-19.87 ± 1.06	3.53 × 10 <sup>12</sup>	141.59 ± 2.73	152.77 ± 2.14	-18.78 ± 0.86
0.30	4.21 × 10 <sup>17</sup>	197.87 ± 1.89	151.16 ± 2.19	78.41 ± 2.10	3.03 × 10 <sup>17</sup>	196.28 ± 3.02	151.20 ± 1.62	75.68 ± 1.36
0.40	9.49 × 10 <sup>19</sup>	224.10 ± 2.08	150.56 ± 2.23	123.46 ± 1.92	5.79 × 10 <sup>19</sup>	221.71 ± 2.65	150.61 ± 2.08	119.35 ± 2.18
0.50	3.57 × 10 <sup>18</sup>	208.22 ± 1.04	150.92 ± 3.04	96.19 ± 0.83	2.75 × 10 <sup>18</sup>	206.95 ± 1.67	150.94 ± 0.97	94.03 ± 2.04
0.60	9.29 × 10 <sup>16</sup>	190.57 ± 3.07	151.35 ± 2.17	65.85 ± 1.62	8.94 × 10 <sup>16</sup>	190.38 ± 3.11	151.35 ± 4.30	65.53 ± 1.69
0.70	7.71 × 10 <sup>16</sup>	189.67 ± 1.74	151.37 ± 2.76	64.30 ± 1.28	7.73 × 10 <sup>16</sup>	189.68 ± 2.39	151.37 ± 2.68	64.32 ± 1.83
average		191.90 ± 1.28	151.36 ± 2.02	68.06 ± 0.68		191.10 ± 1.41	151.37 ± 1.35	66.69 ± 0.92
CS-210								
0.20	2.51 × 10 <sup>18</sup>	207.93 ± 3.64	152.04 ± 2.16	93.20 ± 1.81	1.84 × 10 <sup>18</sup>	206.42 ± 3.64	152.07 ± 1.87	90.64 ± 2.02
0.30	4.48 × 10 <sup>17</sup>	199.53 ± 2.17	152.24 ± 1.89	78.88 ± 1.99	3.79 × 10 <sup>17</sup>	198.73 ± 2.81	152.26 ± 2.14	77.49 ± 1.89
0.40	3.46 × 10 <sup>16</sup>	187.08 ± 2.08	152.55 ± 3.01	57.58 ± 1.15	3.45 × 10 <sup>16</sup>	187.06 ± 2.66	152.55 ± 2.08	57.55 ± 1.80
0.50	1.97 × 10 <sup>16</sup>	184.33 ± 2.64	152.62 ± 2.48	52.88 ± 0.96	2.06 × 10 <sup>16</sup>	184.57 ± 2.57	152.62 ± 1.73	53.29 ± 1.53
0.60	2.36 × 10 <sup>16</sup>	185.22 ± 2.38	152.60 ± 2.06	54.40 ± 1.24	2.51 × 10 <sup>16</sup>	185.52 ± 1.92	152.59 ± 1.82	54.91 ± 1.68
0.70	2.97 × 10 <sup>18</sup>	208.74 ± 1.88	152.02 ± 1.99	94.58 ± 2.07	9.20 × 10 <sup>17</sup>	203.04 ± 2.06	152.15 ± 2.31	84.86 ± 1.79
average		195.47 ± 1.63	152.35 ± 1.58	71.92 ± 1.05		194.22 ± 1.55	152.37 ± 1.61	69.79 ± 1.15
CS-240								
0.20	4.26 × 10 <sup>17</sup>	199.27 ± 2.81	152.23 ± 2.63	78.45 ± 1.28	4.43 × 10 <sup>17</sup>	199.46 ± 2.92	152.22 ± 2.64	78.78 ± 2.08
0.30	1.65 × 10 <sup>17</sup>	194.66 ± 3.13	152.35 ± 2.38	70.57 ± 1.36	1.86 × 10 <sup>17</sup>	195.24 ± 3.04	152.33 ± 2.31	71.57 ± 2.16
0.40	2.14 × 10 <sup>16</sup>	184.73 ± 2.74	152.60 ± 2.32	53.59 ± 1.72	2.47 × 10 <sup>16</sup>	185.42 ± 2.67	152.58 ± 2.39	54.77 ± 1.75
0.50	3.32 × 10 <sup>16</sup>	186.86 ± 2.18	152.54 ± 3.07	57.23 ± 1.63	3.82 × 10 <sup>16</sup>	187.55 ± 2.61	152.52 ± 2.56	58.42 ± 1.68
0.60	5.57 × 10 <sup>16</sup>	189.38 ± 3.04	152.48 ± 2.34	61.55 ± 1.29	5.81 × 10 <sup>16</sup>	189.58 ± 2.18	152.47 ± 2.17	61.89 ± 1.54
0.70	4.87 × 10 <sup>20</sup>	233.60 ± 2.67	152.46 ± 2.18	137.00 ± 1.94	3.44 × 10 <sup>20</sup>	231.90 ± 2.55	151.49 ± 2.81	134.11 ± 2.40
average		198.08 ± 2.26	152.44 ± 2.06	76.40 ± 1.20		198.19 ± 2.30	152.43 ± 2.29	76.59 ± 1.62
CS-270								
0.20	2.90 × 10 <sup>16</sup>	190.38 ± 2.36	156.61 ± 2.27	56.09 ± 1.26	2.74 × 10 <sup>16</sup>	190.10 ± 2.63	156.61 ± 2.18	55.62 ± 1.63
0.30	1.43 × 10 <sup>15</sup>	175.71 ± 2.40	156.99 ± 1.98	31.09 ± 1.18	1.62 × 10 <sup>15</sup>	176.31 ± 2.51	156.98 ± 2.06	32.11 ± 1.24
0.40	6.98 × 10 <sup>15</sup>	183.43 ± 2.81	156.79 ± 2.11	44.25 ± 1.31	7.51 × 10 <sup>15</sup>	183.78 ± 2.46	156.78 ± 2.31	44.85 ± 1.39
0.50	7.15 × 10 <sup>16</sup>	194.78 ± 2.77	156.49 ± 2.06	63.59 ± 1.67	7.08 × 10 <sup>16</sup>	194.73 ± 2.70	156.50 ± 2.13	63.51 ± 1.78
0.60	9.59 × 10 <sup>19</sup>	230.01 ± 2.93	155.68 ± 2.13	123.45 ± 2.18	7.11 × 10 <sup>19</sup>	228.54 ± 2.73	155.71 ± 2.41	120.97 ± 2.31
0.70	5.71 × 10 <sup>26</sup>	306.69 ± 2.68	154.27 ± 1.64	253.16 ± 2.62	2.22 × 10 <sup>26</sup>	302.03 ± 2.88	154.34 ± 2.08	245.30 ± 2.66
average		213.50 ± 2.39	156.14 ± 1.54	95.27 ± 1.25		212.58 ± 2.15	156.15 ± 1.83	93.73 ± 1.32

the OFW method showed a better fitting performance, thus the values calculated by the OFW method were selected.  $\Delta H$  is the total energy of biomass that decomposed into volatiles and solid residues.<sup>14</sup> As can be seen, with the increase of the torrefaction temperature,  $\Delta H$  increased from 191.10 to 194.22, 198.19, and 212.58 kJ/mol. This indicated that the pyrolysis of cornstalk needed more energy after torrefaction. Hemicellulose is less endothermic than lignin and cellulose during the pyrolysis process.<sup>2</sup> By torrefaction pretreatment, the hemicellulose decreased, while more endothermic components such as cellulose and lignin increased, so  $\Delta H$  increased. In addition, torrefaction promoted the aromatization of lignin and made it more difficult to degrade and caused the increase of  $\Delta H$ .<sup>33</sup>  $\Delta G$  represents the increase in the total energy of the system during the formation of substances in the pyrolysis process, and the positive value represents the maximum energy required for the reaction.<sup>34</sup> In this study,  $\Delta G$  increased gradually from 151.37 to 156.15 kJ/mol after torrefaction, and the increasing trend was proportionate to the torrefaction temperature. The increase of  $\Delta G$  represented an increase in the difficulty of the reaction, which indicated that more energy needed to be input into the system after torrefaction. The significant increase of  $\Delta H$  and  $\Delta G$  indicated that torrefaction added to the difficulty of the pyrolysis reaction, which was also verified by the increase of activation energy.  $\Delta S$  is an index to reveal the degree of order of the system. The formation of volatiles

decreases the order of the system, while the formation of char increases the order, and the contribution of these two factors leads to the changes in entropy.<sup>10</sup> The  $\Delta S$  of cornstalk was 66.69 kJ/mol, and it gradually increased for the torrefied samples with elevated torrefaction temperature, especially CS-270, reaching 93.73 kJ/mol. The increase of  $\Delta S$  suggested that torrefaction pretreatment made the structure of cornstalk to become more well organized by gradually favoring lignin as a single component.<sup>35</sup> Combining the results of all thermodynamic properties, it can be inferred that torrefaction increased the difficulty of the pyrolysis reaction in proportion to the torrefied temperature, which was attributed to the changes in the compositions and structure of biomass caused by torrefaction.

#### 4. CONCLUSIONS

The influences of torrefaction on the fundamental characteristics and pyrolysis properties of cornstalk were investigated. It was found that torrefaction promoted the decomposition of hemicellulose and increased the contents of cellulose and lignin. The crystallinity degree increased first and then decreased with elevated torrefaction temperature. In addition, slight torrefaction enhanced the devolatilization and thermochemical reactivity, while serious torrefaction discouraged the volatile release. The OFW model was more accurate in calculating the activation energy, which showed a range of

190–220 kJ/mol. The activation energy and the thermodynamic parameters increased with increasing torrefaction temperature. Torrefaction is a promising pretreatment technology to improve the fuel properties and pyrolysis behavior of cornstalk, which is conducive to the thermochemical conversion of cornstalk as a resource of energy and chemicals.

## AUTHOR INFORMATION

### Corresponding Author

**Jianchun Jiang** – CAF; Key Laboratory of Biomass Energy and Material, Jiangsu Province; Key and Open Laboratory of Forest Chemical Engineering, SFA; National Engineering Laboratory for Biomass Chemical Utilization, Institute of Chemical Industry of Forest Products, Nanjing, Jiangsu 210042, PR China; [orcid.org/0000-0001-6082-6689](https://orcid.org/0000-0001-6082-6689); Email: [lhs\\_ac2011@aliyun.com](mailto:lhs_ac2011@aliyun.com)

### Authors

**Xincheng Lu** – CAF; Key Laboratory of Biomass Energy and Material, Jiangsu Province; Key and Open Laboratory of Forest Chemical Engineering, SFA; National Engineering Laboratory for Biomass Chemical Utilization, Institute of Chemical Industry of Forest Products, Nanjing, Jiangsu 210042, PR China; Co-innovation Center of Efficient Processing and Utilization of Forest Resources, Nanjing Forestry University, Nanjing, Jiangsu 210042, PR China

**Ruting Xu** – CAF; Key Laboratory of Biomass Energy and Material, Jiangsu Province; Key and Open Laboratory of Forest Chemical Engineering, SFA; National Engineering Laboratory for Biomass Chemical Utilization, Institute of Chemical Industry of Forest Products, Nanjing, Jiangsu 210042, PR China

**Kang Sun** – CAF; Key Laboratory of Biomass Energy and Material, Jiangsu Province; Key and Open Laboratory of Forest Chemical Engineering, SFA; National Engineering Laboratory for Biomass Chemical Utilization, Institute of Chemical Industry of Forest Products, Nanjing, Jiangsu 210042, PR China

**Yunjuan Sun** – CAF; Key Laboratory of Biomass Energy and Material, Jiangsu Province; Key and Open Laboratory of Forest Chemical Engineering, SFA; National Engineering Laboratory for Biomass Chemical Utilization, Institute of Chemical Industry of Forest Products, Nanjing, Jiangsu 210042, PR China

**Yanping Zhang** – CAF; Key Laboratory of Biomass Energy and Material, Jiangsu Province; Key and Open Laboratory of Forest Chemical Engineering, SFA; National Engineering Laboratory for Biomass Chemical Utilization, Institute of Chemical Industry of Forest Products, Nanjing, Jiangsu 210042, PR China

Complete contact information is available at:

<https://pubs.acs.org/10.1021/acsomega.2c00047>

### Notes

The authors declare no competing financial interest.

## ACKNOWLEDGMENTS

This work was supported by the National Key R&D Program of China [2019YFD1100604] and the Natural Science Foundation of Jiangsu Province [BK20191135].

## REFERENCES

- (1) Gong, Y.; Zhang, Q.; Zhu, H.; Guo, Q.; Yu, G. Refractory failure in entrained-flow gasifier: vision-based macrostructure investigation in a bench-scale OMB gasifier. *Appl. Energy* **2017**, *205*, 1091–1099.
- (2) Dai, L.; He, C.; Wang, Y.; Liu, Y.; Yu, Z.; Zhou, Y.; Fan, L.; Duan, D.; Ruan, R. Comparative study on microwave and conventional hydrothermal pretreatment of bamboo sawdust: Hydrochar properties and its pyrolysis behaviors. *Energy Convers. Manage.* **2017**, *146*, 1–7.
- (3) Li, J.; Dai, J.; Liu, G.; Zhang, H.; Gao, Z.; Fu, J.; He, Y.; Huang, Y. Biochar from microwave pyrolysis of biomass: A review. *Biomass Bioenergy* **2016**, *94*, 228–244.
- (4) Dai, L.; Wang, Y.; Liu, Y.; Ruan, R.; He, C.; Yu, Z.; Jiang, L.; Zeng, Z.; Tian, X. Integrated process of lignocellulosic biomass torrefaction and pyrolysis for upgrading bio-oil production: A state-of-the-art review. *Renew. Sustain. Energy Rev.* **2019b**, *107*, 20–36.
- (5) Chen, D.; Gao, A.; Ma, Z.; Fei, D.; Chang, Y.; Shen, C. In-depth study of rice husk torrefaction: characterization of solid, liquid and gaseous products, oxygen migration and energy yield. *Bioresour. Technol.* **2018**, *253*, 148–153.
- (6) Chen, D.; Gao, A.; Cen, K.; Zhang, J.; Cao, X.; Ma, Z. Investigation of biomass torrefaction based on three major components: Hemicellulose, cellulose, and lignin. *Energy Convers. Manage.* **2018**, *169*, 228–237.
- (7) Tapasvi, D.; Khalil, R.; Skreiberg, Ø.; Tran, K.-Q.; Grønli, M. Torrefaction of Norwegian birch and spruce: an experimental study using macro-TGA. *Energy Fuel* **2012**, *26*, 5232–5240.
- (8) Chen, W.-H.; Wang, C.-W.; Kumar, G.; Rousset, P.; Hsieh, T.-H. Effect of torrefaction pretreatment on the pyrolysis of rubber wood sawdust analyzed by Py-GC/MS. *Bioresour. Technol.* **2018b**, *259*, 469–473.
- (9) Ru, B.; Wang, S.; Dai, G.; Zhang, L. Effect of torrefaction on biomass physicochemical characteristics and the resulting pyrolysis behavior. *Energy Fuels* **2015**, *29*, 5865–5874.
- (10) Dhyan, V.; Kumar, J.; Bhaskar, T. Thermal decomposition kinetics of sorghum straw via thermogravimetric analysis. *Bioresour. Technol.* **2017**, *245*, 1122–1129.
- (11) Ceylan, S.; Topçu, Y. Pyrolysis kinetics of hazelnut husk using thermogravimetric analysis. *Bioresour. Technol.* **2014**, *156*, 182–188.
- (12) Mallick, D.; Poddar, M. K.; Mahanta, P.; Moholkar, V. S. Discernment of synergism in pyrolysis of biomass blends using thermogravimetric analysis. *Bioresour. Technol.* **2018**, *261*, 294–305.
- (13) Van Soest, P.; Wine, R. H. Use of detergents in the analysis of fibrous feeds. IV. Determination of plant cell-wall constituents. *J. Assoc. Off. Chem.* **1967**, *50*, 50.
- (14) Kaur, R.; Gera, P.; Jha, M. K.; Bhaskar, T. Pyrolysis kinetics and thermodynamic parameters of castor (*Ricinus communis*) residue using thermogravimetric analysis. *Bioresour. Technol.* **2018**, *250*, 422–428.
- (15) Yu, J.; Zhang, M. C.; Shen, Y.; Zhou, Y. G. Thermogravimetric analysis of pyrolysis characteristics of biomass. *J. Shanghai Jiaot. Univ.* **2002**, *36*, 1475–1478.
- (16) Wu, Z.; Wang, S.; Zhao, J.; Chen, L.; Meng, H. Thermochemical behavior and char morphology analysis of blended bituminous coal and lignocellulosic biomass model compound copyrolysis: effects of cellulose and carboxymethylcellulose sodium. *Fuel* **2016**, *171*, 65–73.
- (17) Sadhukhan, A. K.; Gupta, P.; Saha, R. K. Modelling of pyrolysis of large wood particles. *Bioresour. Technol.* **2009**, *100*, 3134–3139.
- (18) Cai, J. M.; Bi, L. S. Kinetic analysis of wheat straw pyrolysis using isoconversional methods. *J. Therm. Anal. Calorim.* **2009**, *98*, 325–330.
- (19) Lu, X.; Jiang, J.; Sun, K.; Sun, Y.; Yang, W. Enhanced antioxidant activity of aqueous phase bio-oil by hydrothermal pretreatment and its structure-activity relationship. *J. Anal. Appl. Pyrol.* **2021**, *153*, 104992.
- (20) Zheng, A.; Zhao, Z.; Chang, S.; Huang, Z.; Zhao, K.; Wei, G.; He, F.; Li, H. Comparison of the effect of wet and dry torrefaction on

chemical structure and pyrolysis behavior of corncobs. *Bioresour. Technol.* **2015**, *176*, 15–22.

(21) Lu, X.; Han, T.; Jiang, J.; Sun, Y.; Yang, W. Comprehensive insights into the influences of acid-base properties of chemical pretreatment reagents on biomass pyrolysis behavior and wood vinegar properties. *J. Anal. Appl. Pyrol.* **2020**, *151*, 104907.

(22) Wang, S.; Dai, G.; Ru, B.; Zhao, Y.; Wang, X.; Xiao, G.; Luo, Z. Influence of torrefaction on the characteristics and pyrolysis behavior of cellulose. *Energy* **2017**, *120*, 864–871.

(23) Tian, X.; Dai, L.; Wang, Y.; Zeng, Z.; Zhang, S.; Jiang, L.; Yang, X.; Yue, L.; Liu, Y.; Ruan, R. Influence of torrefaction pretreatment on corncobs: A study on fundamental characteristics, thermal behavior, and kinetic. *Bioresour. Technol.* **2020**, *297*, 122490.

(24) Mishra, R. K.; Mohanty, K. Pyrolysis kinetics and thermal behavior of waste sawdust biomass using thermogravimetric analysis. *Bioresour. Technol.* **2018**, *251*, 63–74.

(25) Maiti, S.; Purakayastha, S.; Ghosh, B. Thermal characterization of mustard straw and stalk in nitrogen at different heating rates. *Fuel* **2007**, *86*, 1513–1518.

(26) Chutia, R. S.; Katak, R.; Bhaskar, T. Thermogravimetric and decomposition kinetic studies of *Mesua ferrea* L. deoiled cake. *Bioresour. Technol.* **2013**, *139*, 66–72.

(27) Chen, X.; Liu, L.; Zhang, L.; Zhao, Y.; Zhang, Z.; Xie, X.; Qiu, P.; Chen, G.; Pei, J. Thermogravimetric analysis and kinetics of the co-pyrolysis of coal blends with corn stalks. *Thermochim. Acta* **2018b**, *659*, 59–65.

(28) He, Q.; Ding, L.; Gong, Y.; Li, W.; Wei, J.; Yu, G. Effect of torrefaction on pinewood pyrolysis kinetics and thermal behavior using thermogravimetric analysis. *Bioresour. Technol.* **2019**, *280*, 104–111.

(29) Shang, L.; Ahrenfeldt, J.; Holm, J. K.; Bach, L. S.; Stelte, W.; Henriksen, U. B. Kinetic model for torrefaction of wood chips in a pilot-scale continuous reactor. *J. Anal. Appl. Pyrol.* **2014**, *108*, 109–116.

(30) Tong, W.; Liu, Q.; Ran, G.; Liu, L.; Ren, S.; Chen, L.; Jiang, L. Experiment and expectation: Co-combustion behavior of anthracite and biomass char. *Bioresour. Technol.* **2019**, *280*, 412–420.

(31) Burnham, A. K.; Zhou, X.; Broadbent, L. J. Critical review of the global chemical kinetics of cellulose thermal decomposition. *Energy Fuels* **2015**, *29*, 2906–2918.

(32) Zhou, X.; Li, W.; Mabon, R.; Broadbent, L. J. A critical review on hemicellulose pyrolysis. *Energy Technol.* **2016**, *5*, 52–79.

(33) Chen, Z.; Wang, M.; Jiang, E.; Wang, D.; Zhang, K.; Ren, Y.; Jiang, Y. Pyrolysis of torrefied biomass. *Trends Biotechnol.* **2018c**, *36*, 1287–1298.

(34) Yuan, X.; He, T.; Cao, H.; Yuan, Q. Cattle manure pyrolysis process: Kinetic and thermodynamic analysis with isoconversional methods. *Renewable Energy* **2017**, *107*, 489–496.

(35) He, Y.; Chang, C.; Li, P.; Han, X.; Li, H.; Fang, S.; Chen, J.; Ma, X. Thermal decomposition and kinetics of coal and fermented cornstalk using thermogravimetric analysis. *Bioresour. Technol.* **2018b**, *259*, 294–303.